Kinetic and Thermodynamic Studies of the Cross-Bridge Cycle in Rabbit Psoas Muscle Fibers

Yan Zhao and Masataka Kawai
Department of Anatomy, College of Medicine, The University of Iowa, Iowa City, Iowa 52242 USA

ABSTRACT The effect of temperature on elementary steps of the cross-bridge cycle was investigated with sinusoidal analysis technique in skinned rabbit psoas fibers. We studied the effect of MgATP on exponential process (C) to characterize the MgATP binding step and cross-bridge detachment step at six different temperatures in the range 5–30°C. Similarly, we studied the effect of MgADP on exponential process (C) to characterize the MgADP binding step. We also studied the effect of phosphate (Pi) on exponential process (B) to characterize the force generation step and Pi-release step. From the results of these studies, we deduced the temperature dependence of the kinetic constants of the elementary steps and their thermodynamic properties. We found that the MgADP association constant (K_0) and the MgATP association constant (K_1) significantly decreased when the temperature was increased from 5 to 20°C, implying that nucleotide binding became weaker at higher temperatures. K_0 and K_1 did not change much in the 20–30°C range. The association constant of Pi to cross-bridges (K_5) did not change much with temperature. We found that Q_{10} for the cross-bridge detachment step (k_2) was 2.6, and for its reversal step (k_{-2}) was 3.0. We found that Q_{10} for the force generation step (Pi-isomerization step, k_4) was 6.8, and its reversal step (k_{-4}) was 1.6. The equilibrium constant of the detachment step (K_2) was not affected much by temperature, whereas the equilibrium constant of the force generation step (K_4) increased significantly with temperature increase. Thus, the force generation step consists of an endothermic reaction. The rate constant of the rate-limiting step (k_6) did not change much with temperature, whereas the ATP hydrolysis rate increased significantly with temperature increase. We found that the force generation step accompanies a large entropy increase and a small free energy change; hence, this step is an entropy-driven reaction. These observations are consistent with the hypothesis that the hydrophobic interaction between residues of actin and myosin underlies the mechanism of force generation. We conclude that the force generation step is the most temperature-sensitive step among elementary steps of the cross-bridge cycle, which explains increased isometric tension at high temperatures in rabbit psoas fibers.

INTRODUCTION

Muscle contraction is a biological process that involves chemical and mechanical reactions. Chemical reaction generally proceeds faster at higher temperatures, and the processes observed during muscle contraction are not exceptions (Rall and Woledge, 1990). Using this anticipated temperature sensitivity of reactions involved in the cross-bridge cycle, one can probe the thermodynamic and kinetic properties of the cross-bridge cycle. One method of exploration is the temperature jump experiment in which the muscle temperature is increased suddenly and the subsequent tension transient (=time course) is studied (Davis and Harrington, 1987, 1993; Goldman et al., 1987; Bershitsky and Tsaturyan, 1992). The T-jump experiment yielded information on the apparent rate constants, that is, a composite of underlying rate constants of elementary steps. However, because previous T-jump experiments did not study MgATP or phosphate (Pi) dependence of the transient, investigators could not obtain information on the elementary steps of the cross-bridge cycle. The lack of information on elementary steps limits the usefulness of the T-jump study in probing the molecular mechanisms of contraction.

Received for publication 1 February 1994 and in final form 11 April 1994.
Address reprint requests to Dr. Yan Zhao, Department of Anatomy, University of Iowa, Iowa City, IA 52242. Tel.: 319-335-8101; Fax: 319-335-7198. E-mail: MKAWAI@BLUE.WEEG.UIOWA.EDU.

0006-3495/94/10/1655/14 $2.00

It has been known for some time that isometric tension is strongly influenced by temperature in amphibian muscle fibers (Ford et al., 1977; Bressler, 1981) and in mammalian muscle fibers (Ranatunga and Wylie, 1983; Goldman et al., 1987). These observations imply that the kinetic constants of the elementary steps are not equally affected by temperature. A question arises then as to which elementary step is the most temperature-sensitive step. Before answering this question, we must first introduce the elementary steps of the cross-bridge cycle. In our earlier work with sinusoidal analysis in skinned muscle fibers, we have given evidence for a cross-bridge scheme that is consistent with the effects of MgATP, MgADP, and Pi on exponential processes (B), (C), and (D) (Kawai and Halvorson, 1989, 1991; Kawai and Zhao, 1993; Zhao and Kawai, 1993). This scheme is depicted on the next page (see Scheme 1). In step 1a, the substrate (MgATP) binds to the cross-bridge state AM to form a collision complex $AM^{\dagger}S$, and in step 1b, $AM^{\dagger}S$ isomerizes to form the AM*S state (ATP isomerization step). Cross-bridges detach at step 2 to form the Det state. Det is a composite state that includes all detached states (MS, MDP) and "weakly attached" states (AMS, AMDP) described by Brenner et al. (1991). During maximal Ca activation at physiological ionic strength (200 mM), the weakly attached cross-bridges account for 1–2%, and the majority of cross-bridges is either strongly attached or truly detached (Kawai and Zhao, 1993). We found that the apparent rate constant $2\pi d$ reflects the transition between $AM^{\dagger}S$ and AM*S states (step 1b), that the apparent rate constant $2\pi c$ reflects the transition between AM*S and Det

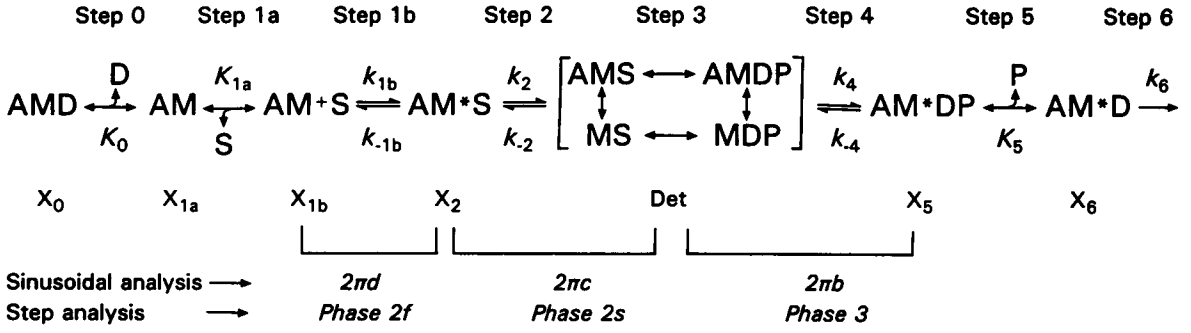

SCHEME 1.

Where A = actin, M = myosin head, S = MgATP, D = MgADP, and P = Pi = phosphate. An asterisk (*) or a dagger (†) identifies the second (and third) conformational state(s). X_i is the steady-state probability of cross-bridges in the respective state.

states (step 2), and that both are sensitive to MgATP and MgADP concentrations. Hydrolysis occurs in step 3, but the product of hydrolysis (ADP, Pi) and the free energy of hydrolysis are all retained on the myosin head. In skinned fiber experiments, this step is not yet resolved primarily because cross-bridges are not attached, and no strong signal comes from step 3.

Cross-bridges first attach to form the weakly attached state AMDP (Brenner et al., 1991), which is based on electrostatic interaction between residues of actin and myosin (Schoenberg, 1988; Sutoh et al., 1991). If the thin filament regulatory unit (3 subunits of troponin, tropomyosin, and 7 actin molecules) is turned on by Ca^{2+}, AMDP isomerizes to form the AM*DP state (Pi-isomerization) in step 4. Our earlier studies (Kawai and Halvorson, 1991; Kawai and Zhao, 1993) as well as others (Dantzig et al., 1992) found that force is generated with this Pi-isomerization; hence, AM*DP is a strongly attached state. The force generation (step 4) is followed by Pi release (step 5) to form the AM*D state. We found that the apparent rate constant $2\pi b$ reflects the transition between Det and AM*DP states (step 4), and is sensitive to Pi, MgATP, and MgADP concentrations. Furthermore, our data are consistent with the hypothesis that the binding of nucleotides (MgATP, MgADP) and Pi is faster than our speed of observation; hence, steps 0, 1a, and 5 can be approximated by equilibria for all practical purposes. Step 6 is the ADP-isomerization/dissociation step, and it is the slowest step of the cross-bridge cycle to limit the ATP hydrolysis rate (rate-limiting step).

With sinusoidal analysis, we were able to determine three association constants and six rate constants of steps 0–5; with the ATP hydrolysis rate measurement, we were able to determine the rate constants of step 6. The above cross-bridge scheme is generally consistent with that derived from solution studies of purified and reconstituted muscle proteins (Taylor, 1979; Eisenberg and Greene, 1980; Geeves et al., 1984).

To find out the temperature sensitivity of elementary steps of the cross-bridge cycle, we studied the effects of MgATP, MgADP, and Pi on exponential processes of tension time course in response to sinusoidal length changes and measured the ATP hydrolysis rate at 6 different temperatures. Our results indicate that step 4 is the most temperature-sensitive step and that it accompanies large enthalpy and entropy changes. These preliminary results have been presented at a Biophysics Society meeting (Zhao and Kawai, 1992).

MATERIALS AND METHODS

Chemicals and solutions

Ethylene glycol-bis(β-amino-ethyl ether) *N',N'*-tetra-acetic acid (H_4EGTA), adenosine 5'-triphosphate (Na_2H_2ATP), adenosine 5'-diphosphate ($Na_{1.5}H_{1.5}$ADP), creatine phosphate (Na_2CP), P^1,P^5-di(adenosine-5')pentaphosphate (A_2P_5), and morpholinopropane sulphonic acid (MOPS) were purchased from Sigma Chemical Co. (St Louis, MO); $CaCO_3$, MgO, NaOH, KOH, KH_2PO_4, K_2HPO_4, and propionic (Prop) acid were from Fisher Scientific (Itasca, IL). Creatine kinase (CK) was purchased from Boehringer Mannheim Chemicals (Indianapolis, IN). All chemicals were analytical grade.

The relaxing solution contained (mM): 6 EGTA, 2 MgATP, 5 free ATP, 8 KPi, 48 KProp, 62 NaProp, and 10 MOPS. The wash solution contained (mM): 0.5 MgATP, 8 KPi, 102 KProp, 74 NaProp, and 10 MOPS. The control activating solution contained (mM): 6 CaEGTA, 5.3 MgATP, 4.7 free ATP, 15 CP, 8 KPi, 35 KProp, 28 NaProp, 10 MOPS, and 160 units/ml CK. The rigor solution contained (mM): 8 KPi, 76 NaProp, 103 KProp, and 10 MOPS. The solution composition for individual experiments is found in Results. In all solutions used for experiments, the total Na concentration was maintained at 75 mM, ionic strength was adjusted to 200 mM with Na/K propionate, and pH was adjusted to 7.00 ± 0.01. EGTA, CaEGTA, and Pi were added as neutral K salts; MgATP and CP were added as neutral Na salts; CK level was doubled for 25°C and quadrupled for 30°C experiments. ADP was added as $Na_{1.5}K_{1.2}$ADP; and free ATP was added as $Na_2K_{1.7}$ATP. Individual concentrations of multivalent ionic species were calculated using our computer program, which assumed multiple equilibria with the following apparent association constants (log values at pH 7.00): CaEGTA = 6.28, MgEGTA = 1.61, CaATP = 3.70, MgATP = 4.00, CaADP = 2.65, MgADP = 2.84, CaCP = 1.15, and MgCP = 1.30.

Fiber preparations

Rabbits were sacrificed by the injection of sodium pentobarbital (150 mg/kg) into an ear vein, and the psoas muscles were exposed and cooled immediately by filling the peritoneal cavity with crushed ice. Skin in the back area was removed, and psoas muscles were also cooled from the back. After 30 min in ice, fiber bundles (approximately 50 mm in length and 3 mm in diameter) were tied to bamboo sticks and excised. Chemical skinning was performed in a solution that contained (mM): 5 EGTA, 2 MgATP, 5 free ATP, 132 NaProp, and 6 imidazole (pH = 7.0) at 2°C for 24 h. The fiber

bundles were then stored at −20°C in a solution that contained (mM): 5 EGTA, 2 MgATP, 5 free ATP, 132 KProp, 6 imidazole (pH = 7.0), and 50% (v/v) glycerol. Cooling the muscle before dissection presumably lowered the activity of proteolytic enzymes present in the fibers. Our skinning solution contained Na^+ instead of K^+ to avoid contraction caused by depolarization of the membrane potential; our solution also contained excess free ATP (5 mM), which helped buffer MgATP against depletion. The combination of these factors contributed to our obtaining exceptionally good quality fibers compared with fibers prepared by the original chemical skinning protocol (Eastwood et al., 1979).

Experimental apparatus

Preparations consisting of two to three fibers were dissected in a petridish filled with the ice-cooled storage solution, and the ends of the fibers were double-knotted. The preparations were then transferred to a muscle chamber, and each end was placed in a hook that is made of J-shaped tungsten wire (125 μm in diameter) with a gap of about 100 μm. One end of the fiber was connected to the length driver, and the other end to the tension transducer assembly. The length driver was made of a Ling 203 vibrator (Ling Dynamic Systems Ltd., Royston Herts, UK) with both photo-electric and magnet-electric length sensors, and similar to the one reported earlier (Kawai and Brandt, 1980). The tension transducer assembly was made of 2-gauge elements (AE 801, SensoNor a.s., Horten, Norway) and stainless-steel tubings, and the assembly had a resonance frequency of 1.5 kHz (Kawai and Brandt, 1980). The fibers were mounted in the relaxing solution. The sarcomere length of the fibers was adjusted to 2.5 μm by optical diffraction using a He-Ne laser (Spectra-Physics, Mountainview, CA), and the length of the preparations (L_0) was measured at this time. L_0 ranged from 4 to 6 mm; the end compliance was not measured. The diameter of each fiber was measured by an ocular micrometer at 200X magnification using Nomarski optics on a Leitz Diavert compound microscope, and the circular cross section was assumed to calculate the cross sectional area of the fibers.

Experimental procedure

The fiber preparation in the relaxing solution was rinsed with wash solution to remove EGTA. The wash solution was then replaced with that with the same composition as the activating solution except for the omission of CaEGTA. The baseline record of the complex modulus was collected at this time, and then concentrated CaEGTA was added to the final concentration of 6 mM (pCa 4.82). When a steady tension developed, an experimental record of the complex modulus was collected. Thereafter, the fiber was relaxed. In a series of experiments that studied the MgATP effect, the above sequence was repeated for solutions that contained different concentrations of MgATP. The MgADP and Pi studies followed the same sequence. At the beginning and end of each series of experiments, the preparation was tested with the control activating solution to examine the reproducibility of the data. Data from any preparation that exhibited less then 80% control tension were not used for analysis. At the end of each experiment, rigor was induced (see Kawai and Zhao (1993) for this procedure), and the complex modulus of the rigor state was collected; all of the experimental data were corrected against the rigor data as described in Appendix 1 of our earlier report (Kawai and Brandt, 1980). This procedure removes the artificial frequency response of the tension transducer assembly caused by visco-elasticity and mass of the assembly.

The complex modulus $Y(f)$ is defined as the ratio of stress change to strain change expressed in the frequency domain. $Y(f)$ is fitted to an equation consisting of four exponential processes (Zhao and Kawai, 1993):

$$Y(f) = H + \underbrace{A/(1 + a/fi)}_{\text{Process (A)}} - \underbrace{B/(1 + b/fi)}_{\text{Process (B)}} + \underbrace{C/(1 + c/fi)}_{\text{Process (C)}} + \underbrace{D/(1 + d/fi)}_{\text{Process (D)}} \quad (1)$$

$$Y_\infty \equiv H + A - B + C + D, \quad (2)$$

where $i = \sqrt{-1}$ and f is the frequency of sinusoidal length oscillation. Data were collected in 18 discrete frequencies ranging from 0.25 to 350 Hz. This frequency range corresponds to 0.45–600 ms in time domain analysis. Peak-to-peak amplitude was fixed to 0.250 ± 0.003% L_0 in all frequencies. This length change corresponds to ±1.6 nm per half sarcomere. We denote

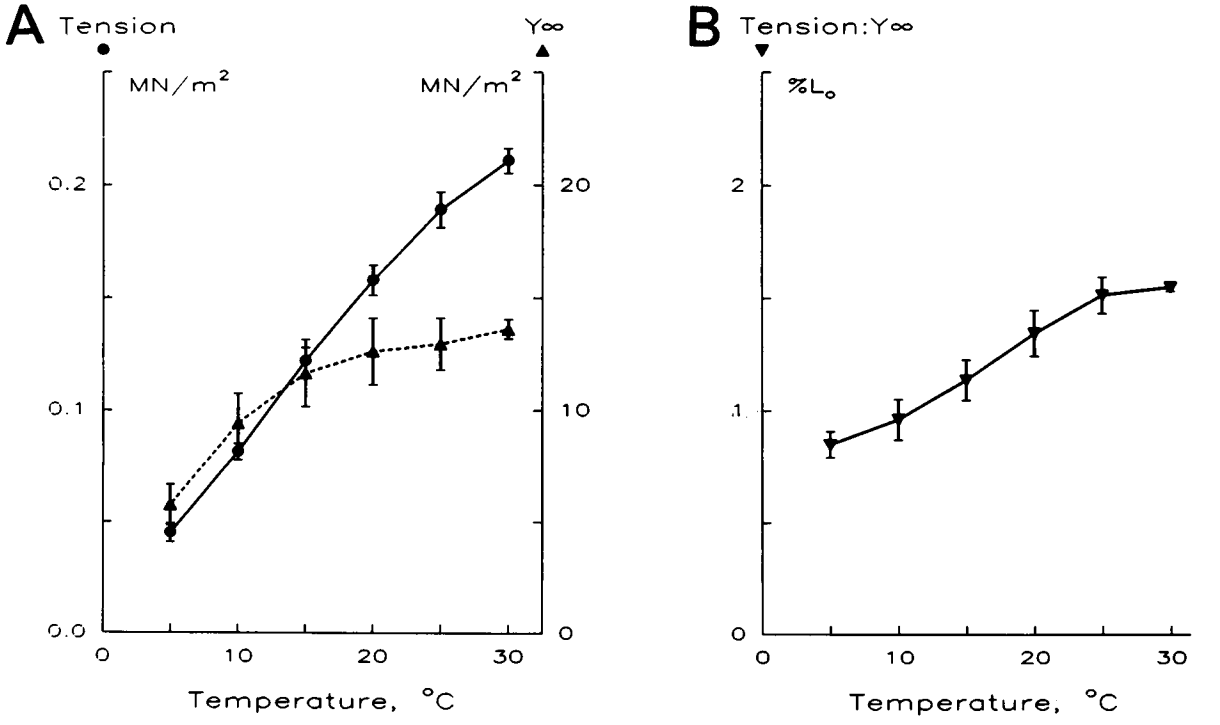

FIGURE 1 (*A*) Isometric tension (●) and stiffness (▲) are plotted against temperature. (*B*) The ratio of tension to stiffness (T:Y_∞) is plotted against temperature. The average of nine experiments is shown with SEM error bars.

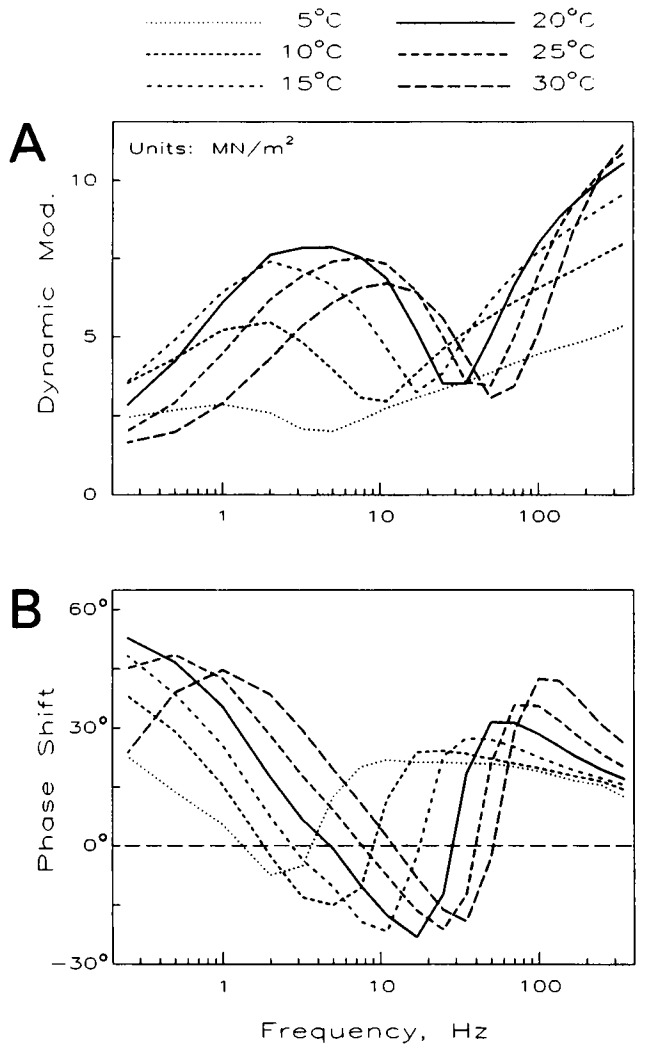

FIGURE 2 (*A*) The dynamic modulus vs. frequency at six different temperatures (indicated on top of the figure). (*B*) Phase shift versus frequency at six different temperatures. Phase shift is positive on phase advance (tension change leads length change), and negative on phase delay (tension change lags behind length change). Each curve represents the average of nine experiments.

characteristic frequencies of respective processes by *a*, *b*, *c*, *d* and their magnitudes by *A*, *B*, *C*, *D*. *H* is the modulus extrapolated to the zero frequency. 2π times characteristic frequencies represent apparent (observed) rate constants. The parameters of 4 exponential processes were found by a nonlinear data-fitting procedure similar to the one described in an earlier report (Kawai and Brandt, 1980). Y_∞ defined in Eq. 2 is the complex modulus extrapolated to the infinite frequency, and it does not have an imaginary part. This quantity is referred to as "stiffness" in our reports, and it is generally assumed to be proportional to the number of attached cross-bridges. Y_∞ corresponds to phase 1 of step analysis (Huxley and Simmons, 1971; Heinl et al., 1974), process (D) corresponds to the fast component of phase 2, process (C) to the slow component of phase 2, process (B) to phase 3, and process (A) to phase 4 (see scheme 1). The details of the sinusoidal analysis method were published previously (Kawai and Brandt, 1980).

We measured the ATP hydrolysis rate at six different temperatures as described (Güth and Wojciechowski, 1986; Zhao and Kawai, 1993). The rate constant of step 6 (k_6) was calculated based on Eq. 3:

$$\text{ATP hydrolysis rate} = k_6[\text{AM*D}], \quad (3)$$

where [AM*D] is the concentration of the AM*D state defined in scheme 1.

RESULTS

Effect of temperature on isometric tension and stiffness

The isometric tension and stiffness in the control activating solution at different temperatures are shown in Fig. 1 *A*. Isometric tension increased almost proportionately to the centigrade (°C) temperature. At low temperatures (5–10°C), stiffness increased parallel to tension; at high temperatures (15–30°C), the stiffness increase was less than the tension increase. The tension to stiffness ratio increased from 0.85 to 1.55% L_0 with an increase in the temperature (Fig. 1 *B*).

Effect of temperature on exponential processes

Fig. 2 *A* demonstrates the dynamic modulus plotted against frequency, and Fig. 2 *B* shows the phase shift plotted against frequency at six different temperatures. The data were obtained from the same experiments referenced in Fig. 1. From Fig. 2, it is clear that the characteristic frequencies that give minimum and maximum values in the dynamic modulus (Fig. 2 *A*) and phase shift (Fig. 2 *B*) increase with an increase in temperature, indicating that all of the apparent rate constants increased with temperature. The data were fitted to

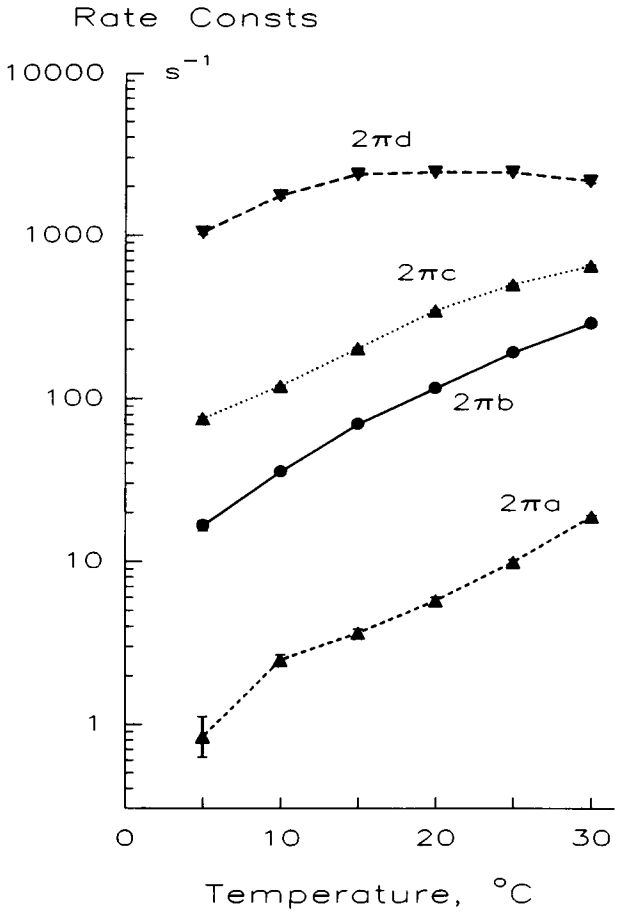

FIGURE 3 Four apparent rate constants are plotted against temperature on a logarithmic scale. The data are the average of nine experiments with SEM error bars.

Eq. 1, and parameters of exponential processes were deduced. Fig. 3 illustrates the effect of temperature on four apparent rate constants. This figure demonstrates that $2\pi a$, $2\pi b$, and $2\pi c$ increase with temperature significantly, whereas the increase in $2\pi d$ is less. The Q_{10} of these rate constants are listed in Table 1. This Table demonstrates that Q_{10} for $2\pi b$ is largest and 3.07, followed by Q_{10} for $2\pi a$ and $2\pi c$. Q_{10} for $2\pi d$ is smallest and 1.5.

The effect of MgATP on exponential processes (C) at different temperatures

To examine whether the elementary steps involved in the MgATP binding and the cross-bridge detachment steps are sensitive to the temperature change, we studied the effect of MgATP on exponential process (C) at six different temperatures. The effect of MgATP was studied in the concentration range from 0.1 to 10 mM. Individual MgATP solutions were created by appropriately mixing two solutions 0*S* and 10*S*, where *S* denotes the millimolar concentration of $MgATP^{2-}$. 0*S* solution contained (mM): 5.0 free ATP, 40 KProp, and 38 NaProp. 10*S* solution contained (mM): 10.6 MgATP, 4.4 free ATP, 30 KProp, and 18 NaProp. In addition, both solutions contained (mM): 6 CaEGTA (pCa 4.82–4.84), 8 KPi, 15 CP, 10 MOPS, and 160 units/ml CK. The high Pi concentration (8 mM) was chosen because, at this concentration, more cross-bridges were distributed among the states AM, $AM^{\dagger}S$, AM*S, and Det (Scheme 1), so that a better resolution of processes (C) was obtained. The resulting complex modulus data were fitted to Eq. 1, and the rate constant $2\pi c$ was obtained. Because the observed rate constant $2\pi d$ was scattered (Table 1) and not quite a hyperbolic function of MgATP in all temperature ranges we studied, we did not deduce the rate constant of step 1b in the present report. In Fig. 4, the apparent rate constant $2\pi c$ is plotted against MgATP concentration at six different temperatures. These plots reveal that the MgATP dependence of $2\pi c$ is hyperbolic: $2\pi c$ increased at low millimolar concentrations, and it approached saturation by 5–10 mM. Such MgATP dependence can be explained by Eq. 4, which was derived from Scheme 1 that lacks the $AM^{\dagger}S$ state (Kawai and Halvorson, 1989):

$$2\Pi c = \frac{K_1 S}{1 + K_0 D + K_1 S} k_2 + k_{-2}, \qquad (4)$$

where *S* represents the $MgATP^{2-}$ (substrate) concentration, *D* represents the $MgADP^{-}$ concentration, and K_1 represents the association constants of MgATP to cross-bridges. For

TABLE 1 Q_{10} of the apparent rate constants

Apparent rate constants	Q_{10}	Temperature range (°C)
$2\pi a$	2.53 ± 0.07	10–25
$2\pi b$	3.07 ± 0.07	10–25
$2\pi c$	2.64 ± 0.02	10–25
$2\pi d$	1.5 ± 0.4	10–25

± SEM for N = 7–9.

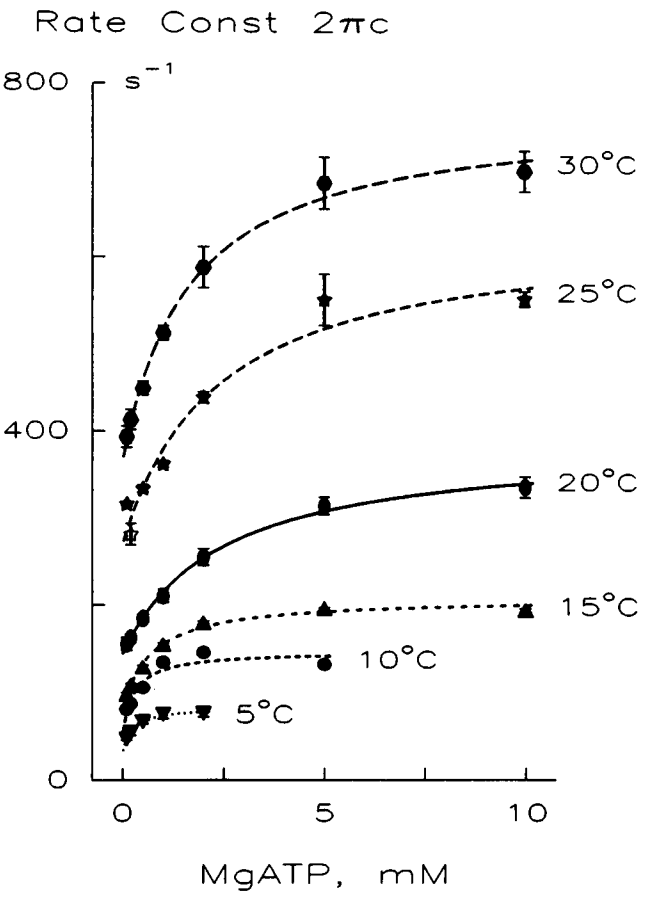

FIGURE 4 The apparent rate constant $2\pi c$ is plotted against MgATP concentration at six different temperatures. The data are the average of 7 (5°C), 8 (10°C), 10 (15°C), 7 (20°C), 8 (25°C), and 7 (30°C) experiments with SEM error bars. The curved lines are based on Eq. 4 and the best-fit parameters. The units of the ordinate are s^{-1}.

experiments that used CP/CK, the ADP concentration is less than 20 μM (Meyer et al., 1985); hence it is assumed $K_0 D = 0$. K_1 is a composite of step 1a and 1b in Scheme 1. k_2 represents the forward rate constant of the cross-bridge detachment step 2, k_{-2} represents the backward rate constant of the detachment, and $K_2 = k_2/k_{-2}$ is the equilibrium constant. These kinetic constants are shown in Scheme 1. The data in Fig. 4 were fitted to Eq. 4, and theoretical projections are reflected in the figure by the curved lines. These lines reveal that both the intercept to 0 MgATP concentration (k_{-2}) and the increment to a large MgATP concentration (k_2) increased with temperature. They further reveal that the half-saturation point ($=1/K_1$) increased in the low temperature range (5–20°C). At 5 and 10°C, we noticed a decline of $2\pi c$ at high MgATP concentrations (substrate inhibition); hence these points were not used for data fitting. The kinetic constants were deduced from these fittings and plotted in Fig. 5 as functions of $1000/T$, where T is the absolute temperature. The Celsius temperature (°C) is shown at the top of the figure. As seen in Fig. 5 *A*, the MgATP binding constant K_1 significantly decreased when the temperature was increased from 5 to 20°C, implying that MgATP binding became

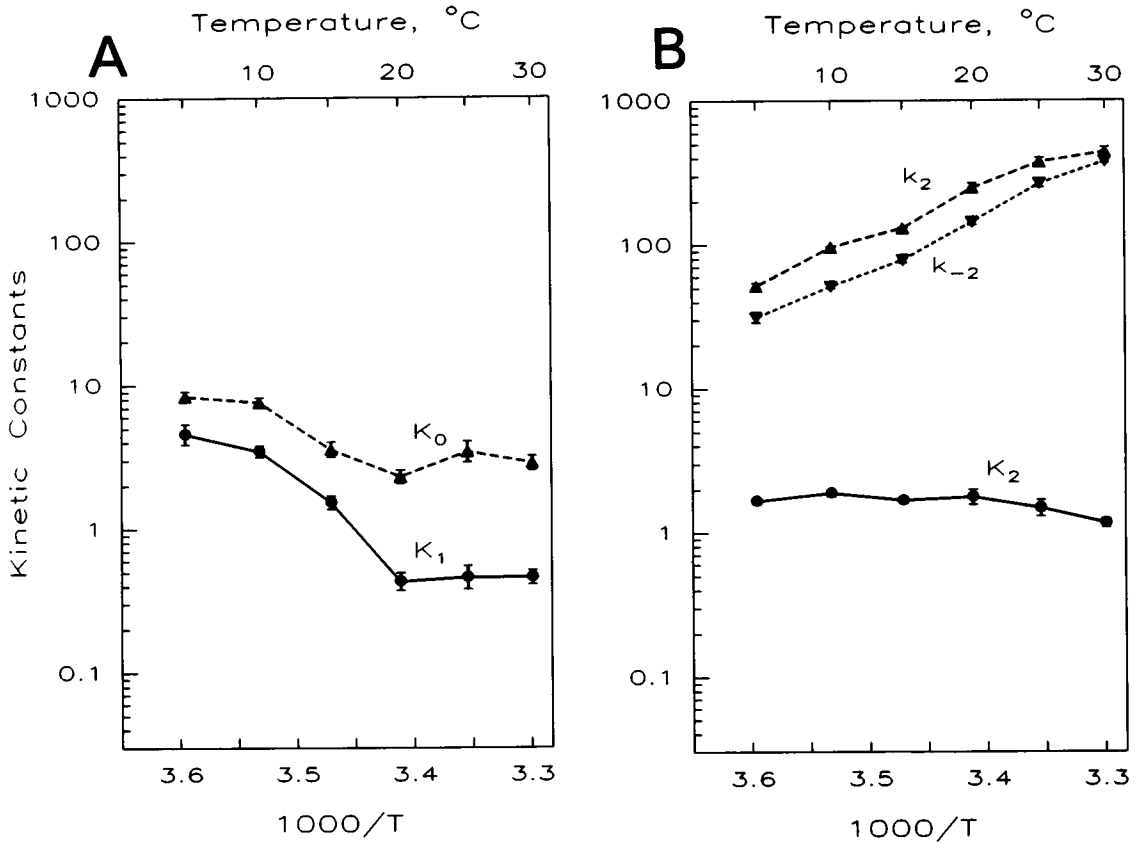

FIGURE 5 The temperature dependence of the kinetic constants of steps 0–2. The data were averaged and plotted with SEM error bars on a logarithmic scale. (*A*) The association constants K_0 for MgADP (based on the MgADP study on $2\pi c$, N = 4–8) and K_1 for MgATP (based on the MgATP study on $2\pi c$, N = 5–7) are plotted against temperature. (*B*) The rate constants and equilibrium constant of cross-bridge detachment step 2 are plotted against temperature. The data were based on the MgATP study on $2\pi c$ (N = 5–7). The units of the association constants K_0 and K_1 are mM^{-1}; the rate constants k_2 and k_{-2} are s^{-1}; the equilibrium constant K_2 is unitless.

weaker at higher temperatures. K_1 did not change much in the high temperature range (20–30°C). In Fig. 5 *B*, it is seen that the cross-bridge detachment rate constant k_2 and its reversal k_{-2} increased similarly with temperature. Because they increase in parallel in logarithmic plots, the equilibrium constant K_2 did not change much with temperature.

The effect of MgADP on exponential process (C) at different temperatures

To characterize the temperature dependence of the association constant (K_0) of MgADP to the cross-bridge state AM (step 0, Scheme 1), the total MgADP concentration was changed in the 0–8 mM range, and the rate constant of process (C) was studied at six different temperatures. In these studies, the MgATP concentration was fixed at 5 mM. Individual solutions were created by appropriately mixing two extreme solutions 0*D* and 8*D*, where *D* denotes the total millimolar concentration of MgADP. 0*D* solution contained (mM): 0.3 $MgProp_2$, 66 NaProp, and 69 KProp. 8*D* solution contained (mM): 8 ADP, 3.5 $MgProp_2$, 54 NaProp, and 47 KProp. In addition, both solutions contained (mM): 6 CaEGTA (pCa 4.54–4.64), 6.1 MgATP, 0.2 A_2P_5, 8 KPi, and 10 MOPS. Mg^{2+} concentration was maintained at 1 mM. CP and CK were deleted from the saline, and 0.2 mM A_2P_5 was added to inhibit adenyl kinase activity (Feldhaus et al., 1975). In Fig. 6, the apparent rate constant $2\pi c$ is plotted against the $MgADP^-$ concentration at different temperatures. We chose to use the $MgADP^-$ concentration on the abscissa rather than the total ADP concentration as we did previously (Kawai and Halvorson, 1989; Zhao and Kawai, 1993), because the Mg bound form is the most likely species that binds to the nucleotide binding site of myosin. At 1 mM Mg^{2+} concentration, about 40% of ADP chelates Mg. Because of this, the estimated K_0 value increased to 2.5 times the previously reported value (Kawai and Halvorson, 1989; Zhao and Kawai, 1993). The results were fitted to Eq. 4 to deduce K_0 by utilizing K_1 obtained from the MgATP study. K_0 is plotted in Fig. 5 *A* as a function of temperature. K_0 decreased when temperature was increased from 5 to 20°C, then K_0 increased slightly when the temperature was increased from 20 to 30°C. As seen in Fig. 5 *A*, temperature affected K_0 and K_1 similarly.

The effect of phosphate on exponential process (B) at different temperatures

To characterize the temperature dependence of Pi-isomerization (force generation) step 4 and Pi-release step 5, we

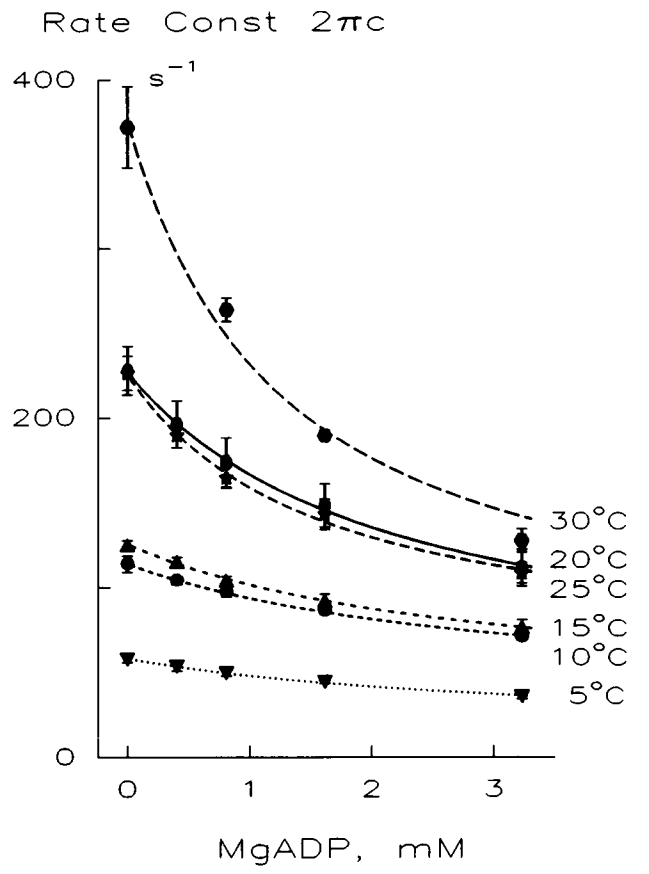

FIGURE 6 The apparent rate constant $2\pi c$ is plotted against the $MgADP^-$ concentration at six different temperatures. The data are the average of four to eight experiments with SEM error bars. The curves are based on Eq. 4 and the best-fit parameters. The units of the ordinate are s^{-1}.

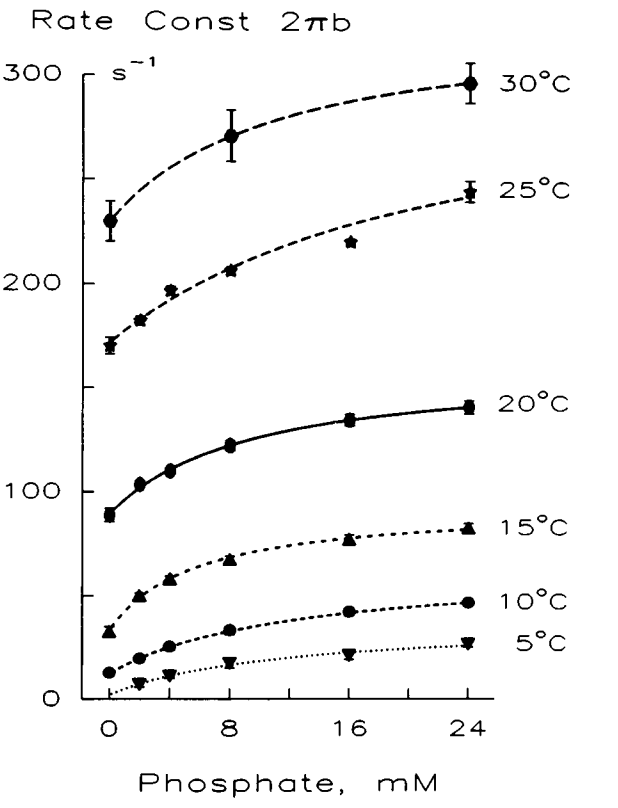

FIGURE 7 The apparent rate constant $2\pi b$ is plotted against Pi concentration at six different temperatures. Symbols indicate the averaged values, and error bars indicate SEM. The numbers of observations are 8 (5°C), 9 (10°C), 10 (15°C), 11 (20°C), 8 (25°C), and 7 (30°C). The curved lines are based on Eq. 5 and the best-fit parameters. The units of the ordinate are s^{-1}.

studied the effect of Pi on exponential process (B). When the apparent rate constant $2\pi b$ was plotted against the Pi concentration (Fig. 7), the plot was hyperbolic (concave downward). This relationship was fitted to Eqs. 5 and 6 ($D = 0$ is assumed), which is based on Scheme 1.

$$2\pi b = \sigma k_4 + \frac{K_5 P}{1 + K_5 P} k_{-4}, \tag{5}$$

$$\sigma = \frac{K_2 K_1 S}{1 + K_0 D + (1 + K_2) K_1 S}. \tag{6}$$

The derivation of Eqs. 5 and 6 was given in our previous report (Kawai and Halvorson, 1991). It is clear from Eq. 5 that the intercept to the ordinate (Pi = 0) in Fig. 7 represents the rate constant of Pi-isomerization step (k_4) multiplied by the constant factor σ (Eq. 6). σ takes a value between 0.44 and 0.62 under our experimental conditions. The increment to the large Pi concentration represents the rate constant of the reverse isomerizatiuon step (k_{-4}). The Pi concentration at the half-saturation point is the dissociation constant of Pi from the cross-bridge AM*DP state (step 5), and its reciprocal is the association constant K_5. In Fig. 7, the curved lines represent theoretical projections based on Eq. 5. An examination of Fig. 7 reveals that the zero intercept (σk_4) increases significantly with temperature, whereas the increment to a large Pi concentration (k_{-4}) is not as large. The half-saturation point appears not to change much with temperature. σ was calculated based on Eq. 6 with K_1 and K_2 obtained for the MgATP study and $S = 5$ mM.

The kinetic constants were deduced by fitting the data to Eq. 5, and they are plotted in Fig. 8 against $1000/T$. As seen in this figure, the rate constant of Pi-isomerization (force generation) step (k_4) increased significantly with an increase in the temperature, whereas the rate constant of its reversal step (k_{-4}) did not change much with temperature. This resulted in a large increase in the equilibrium constant K_4 with temperature (Fig. 8). The association constant of Pi to cross-bridges K_5 did not change much with temperature; the effect was a factor of 2 at the most (Fig. 8). We found Q_{10} for k_4 was 6.8, and the corresponding activation energy was 135 kJ/mol (Table 2, Fig. 11). Q_{10} for k_{-4} was 1.6, and the corresponding activation energy was 33 kJ/mol.

The effect of temperature on cross-bridge distribution

Based on the equilibrium constants we obtained, we calculated the steady-state distribution (probability) of cross-

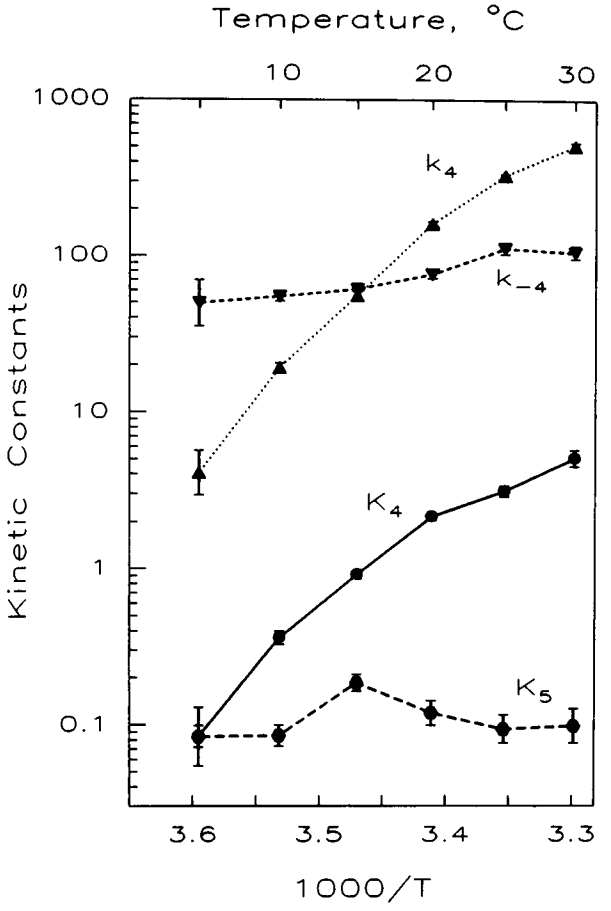

FIGURE 8 The temperature sensitivity of the kinetic constants of steps 4 and 5. The data were based on the phosphate study on $2\pi b$, and averaged and plotted with SEM error bars on a logarithmic scale. The units of k_4 and k_{-4} are s^{-1}, K_4 unitless, and K_5 mM^{-1}.

bridges among various states at different temperatures (Fig. 9) based on Eqs. 7–13 (Kawai and Halvorson, 1991):

$$X_0 = K_0DK_5P/M \quad (7)$$

$$X_1 = K_5P/M \quad (8)$$

$$X_2 = K_1SK_5P/M \quad (9)$$

$$X_{34} = K_1SK_2K_5P/M \quad (10)$$

$$X_5 = K_1SK_2K_4K_5P/M \quad (11)$$

$$X_6 = K_1SK_2K_4/M \quad (12)$$

where

$$M \equiv K_1SK_2K_4 + K_5P[1 + K_0D + K_1S(1 + K_2 + K_2K_4)] \quad (13)$$

The calculation was based the standard activating condition, which included 5 mM MgATP and 8+1 mM Pi. 1 mM Pi was added to account for endogenous Pi (Kawai and Zhao, 1993). In Fig. 9, the probability for the AMD state is not shown, because it is less than 0.1% when the MgADP concentration is less than 20 μM in the presence of CP/CK (Meyer et al., 1985).

Fig. 9 demonstrates that the number of detached cross-bridges is largest at 5°C and gradually decreases at higher temperature. The number of attached tension-generating states (AM*DP and AM*D) increases significantly with temperature. They account for 35% at 10°C, 69% at 20°C, 83% at 30°C, and they approximately scale with isometric tension (Fig. 1 *A*). The exact correlation between isometric tension and stiffness (Y_∞) with temperature elevation requires a deduction of force per cross-bridge state (Kawai and Zhao, 1993) at each temperature and will be addressed in a subsequent paper.

The effect of temperature on the rate-limiting step

We have shown that step 6 (isomerization of AM*D state to result in the AMD or AM state) limits the ATP hydrolysis rate in the near isometric condition in skinned rabbit psoas muscle fibers (Kawai and Halvorson, 1991; Kawai and Zhao, 1993). To determine whether this rate-limiting step is temperature-sensitive, we measured the ATP hydrolysis rate at six different temperatures. Both relaxing and activating solutions contained (mM): 15 Na_2KPEP, 8 KPi, 10 NaN_3, 28 NaProp, 10 MOPS (pH adjusted to 7.00), 1.2 NADH, 0.18 A_2P_5, 92 units/ml PK, and 130 units/ml LDH. In addition, the activating solution contained (mM): 6 CaEGTA (pCa 4.58), 6.07 MgATP, 1.39 $MgProp_2$, and 33 KProp; the relaxing solution contained (mM): 0.108 CaEGTA, 5.89 EGTA (pCa 8.00), 6.01 MgATP, 1.68 $MgProp_2$, and 32 KProp.

As shown in Fig. 10, the ATP hydrolysis rate (*filled circles*) increased significantly with an increase in the temperature. Because the hydrolysis rate is the product of the rate constant of the rate-limiting step k_6 and the number of cross-bridges in the AM*D state (Eq. 3), we divided the hydrolysis rate by the calculated cross-bridge number in the AM*D state (Eq. 12) at each temperature. The total myosin head concentration in skinned fibers was assumed to be 0.2 mM (Tregear and Squire, 1973). The result was plotted in triangles and a dotted line in Fig. 10. It is clear from this figure that k_6 is little sensitive to the temperature with Q_{10} of 1.1 (Table 2). Thus, we concluded that the increase in the ATP hydrolysis rate with temperature elevation is primarily caused by the increased cross-bridge number in the AM*D state at higher temperature, and not by k_6.

Activation energy and standard enthalpy and entropy changes

Based on Arrhenius equation (Eq. 14), we calculated the activation energy (E_a) of each step in the cross-bridge cycle (Table 2).

$$k = Q\exp(-E_a/RT) \quad (14)$$

where k = the rate constant of elementary step, R = gas constant, and Q = frequency factor. The calculation was based on the experimental data obtained in the temperature range between 10 and 25°C, because data deviated from Eq. 14 at 5 and 30°C (Figs. 5, 8, and 10). We also calculated

TABLE 2 The rate constants of elementary steps and their temperature sensitivity

Rate constants	Value at 20°C (s^{-1})	Q_{10}	Activation energy E_a (kJ/mol)	Frequency factor Q (s^{-1})	Temperature range (°C)
k_2	250 ± 20	2.6	66	1.4×10^{14}	10–25
k_{-2}	143 ± 7	3.0	77	8.7×10^{15}	10–25
k_4	161 ± 5	6.8	135	1.5×10^{26}	10–25
k_{-4}	77 ± 5	1.6	33	5.9×10^{7}	10–25
k_6	16 ± 1	1.1	7	16.4	10–25*

The rate constants were fitted to Eq. 14 to deduce E_a and Q in the specific temperature range.
±SEM for N = 7–9.
* Excludes 15°C.

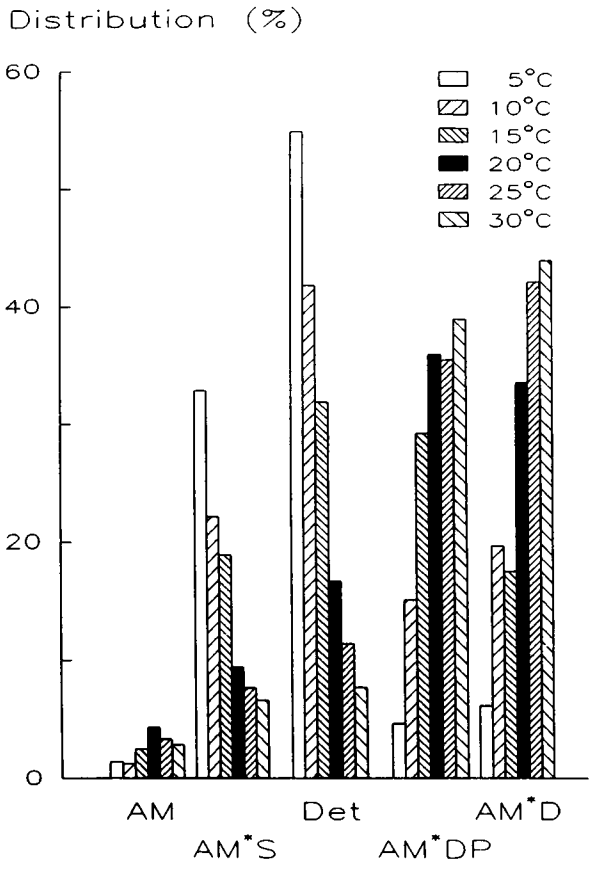

FIGURE 9 Distribution (probability) of cross-bridges at six different temperatures is based on Eqs. 7–13 at 5 mM MgATP and 9 mM Pi. The distribution of cross-bridges in the AMD state is small (<0.1%) and not shown.

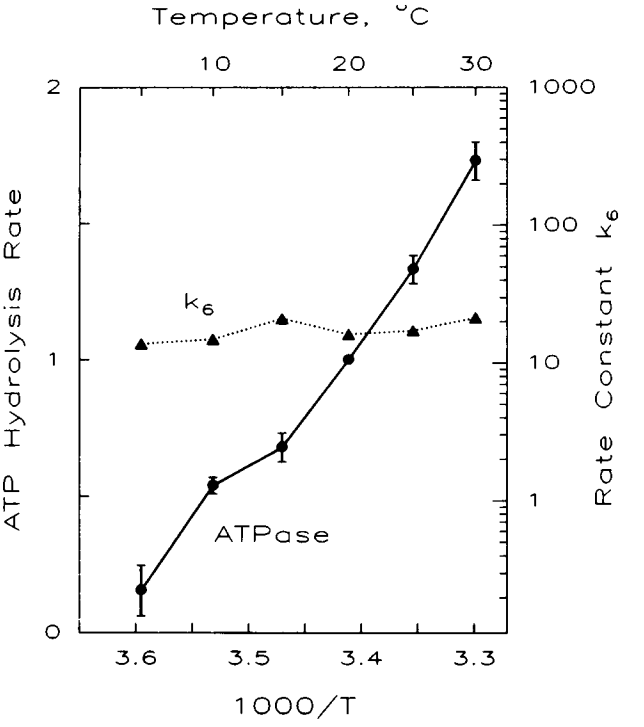

FIGURE 10 The ATP hydrolysis rate (●) and rate constant k_6 (▲) are plotted against temperature. The data are averages of 6 (5°C), 6 (10°C), 6 (15°C), 11 (20°C), 9 (25°C), and 9 (30°C) with SEM error bars. The ATP hydrolysis rate was normalized to the value at 20°C.

the standard enthalpy change ($\Delta H°$) and the standard entropy change ($\Delta S°$) for each step by using Van't Hoff equation (Eq. 15).

$$\ln K = \Delta S°/R - \Delta H°/RT \quad (15)$$

$$\Delta G° = -RT \ln K, \quad (16)$$

where K = equilibrium constant and $\Delta G°$ is the standard free energy change. The results are listed in Table 3. Because the slope of the nucleotide association constants K_0 and K_1 was not continuous, we calculated the enthalpy change and the entropy change of K_0 and K_1 at low and high temperature ranges. As seen in this table, $\Delta H°$ for K_4 is +103 kJ/mol; hence the force generation step 4 is an endothermic reaction (i.e., absorbs heat), and it has a large entropy increase corresponding to 357 J/mol/deg. In contrast, the cross-bridge detachment step 2 does not accompany a large enthalpy or entropy change. The nucleotide-binding steps 0 and 1 are exothermic and accompany moderate entropy changes. The phosphate-binding step 5 accompanies a small entropy increase.

DISCUSSION

Isometric tension and stiffness

Isometric tension increased almost proportionately to the centigrade temperature (Fig. 1 *A*). At a low temperature, stiffness increased parallel to tension; at a high temperature, the stiffness increase was less than the tension increase. These results are generally consistent with previous reports

TABLE 3 The equilibrium constants and their standard enthalpy and entropy changes

Equilibrium constants	Value at 20°C	Q_{10}	Enthalpy change ΔH°(kJ/mol)	Entropy change ΔS°(J/mol/deg)	Temperature range (°C)
K_0	2.3 ± 0.2	0.3	−83	−219	10–20
		1.2	16	121	20–30
K_1	0.43 ± 0.06	0.12	−144	−440	10–20
		1.1	5	67	20–30
K_2	1.77 ± 0.2	0.9	−10	−29	10–25
K_4	2.16 ± 0.11	4.3	103	357	10–25
K_5	0.12 ± 0.02	1.1	7	64	10–25

The equilibrium constants were fitted to Eq. 15 to deduce ΔH° and ΔS° in the specific temperature range. The units for K_0, K_1, and K_5 are mM^{-1}; K_2 and K_4 are unitless.
±SEM for N = 5–9.

on frog tibialis anterior muscle fibers (Ford et al., 1977), on frog and toad sartorius muscles (Bressler, 1981), and on rabbit psoas muscle fibers (Goldman et al., 1987).

The tension to stiffness ratio of ~1.0% (Fig. 1 *B*) is the typical value of skinned psoas fibers. The ratio compares with 1.0% (Chase et al., 1993) in the experiment that controlled the sarcomere length in glycerinated psoas fibers at 10–13°C. Our extrapolated value for 11.5°C is 1.0% (Fig. 1 *B*), which agrees well with the result of Chase et al. (1993), indicating that the end compliance is not a contributing factor in our measurements. In intact frog muscle fibers, the ratio is 0.5–0.7% (Huxley and Simmons, 1971; Ford et al., 1977)at low temperature (0–4°C). The cause of this disagreement between intact and skinned fibers is not immediately obvious.

Exponential processes

Our temperature study on exponential processes showed that the apparent rate constants $2\pi a$, $2\pi b$, and $2\pi c$ significantly increase with temperature increase, whereas $2\pi d$ does not change much with temperature (Fig. 3). We found that Q_{10} of $2\pi a$, $2\pi b$, $2\pi c$, and $2\pi d$ is 2.53, 3.07, 2.64, and 1.5, respectively (Table 1). These results are strikingly similar to the results of Abbott and Steiger (1977). They studied the tension transients after a step length change on skinned rabbit psoas muscle fibers as a function of temperature. They observed four exponential processes in the tension transients and named them phases 1, 2, 3, and 4 in the order of decreasing speed. These correspond to our exponential processes (D), (C), (B), and (A), respectively. They found that the rate constants of phases 2–4 are temperature-sensitive, whereas the rate constant of phase 1 is only slightly temperature-sensitive (Abbott and Steiger, 1977, Fig. 8). In intact frog muscle fibers, Ford et al. (1977) reported Q_{10} of phase 2 ($2\pi c$ and $2\pi d$ combined) to be 1.85 in the temperature ranging from −0.1 to 8.1°C, which compares with our Q_{10} of 2.64 ($2\pi c$) and 1.5 ($2\pi d$). It is possible that the small Q_{10} with $2\pi d$ may be related to the finite frequency range that we used. Because of this limitation, we did not include the results from $2\pi d$ in the following analysis of elementary steps of the cross-bridge cycle. The apparent rate constant $2\pi a$ changes similarly with $2\pi b$ and $2\pi c$ with temperature. This is expected, because $2\pi a$ represents filament sliding or sarcomere rearrangement during muscle contraction (Tawada and Kawai, 1990).

The previous studies focused on the temperature sensitivity of an apparent (=observed) rate constant, which is a function of underlying chemical reactions. In this report, we were able to resolve elementary steps of the cross-bridge cycle and their individual temperature sensitivity. Each step is discussed in the following section.

Nucleotide-binding steps

According to a recent crystallographic description of myosin S-1 (Rayment et al., 1993a), the nucleotide-binding region forms a pocket in the N-terminal 25 kDa domain (see also Szilagyi et al., 1979). Our results showed that MgATP binding (K_1) becomes weaker with temperature increase from 5 to 20°C; hence the binding reaction is exothermic (Fig. 5 *A*). This observation implies that the contour of the nucleotide-binding site may change with temperature. One possibility is that the temperature change directly causes a shape change in the myosin head. The fact that temperature effect on K_1 saturates at 20–30°C (Fig. 5 *A*) may be consistent with this mechanism.

A second possibility is that the shape change is coupled with the interaction of actin and myosin. In a separate study, we found that the nucleotide association constants (K_0 and K_{1a}) increased as isometric tension was decreased either by 2,3-butandione monoxime (BDM) (Zhao and Kawai, 1994) or by partial troponin C extraction (Zhao et al., 1994). All of these studies indicate that an increase in the number of (strongly) attached cross-bridges results in a decrease in the nucleotide-binding constant, suggesting that the degree of cooperative activation of the thin filament regulatory unit may be involved in modulating the nucleotide-binding step. Modulation of the nucleotide-binding site by actin binding to the myosin head was demonstrated and discussed by Kodama (1985) based on free energy change of interaction of nucleotide and actin binding sites (see also Greene and Eisenberg, 1980).

A third possibility, that the ATP-regenerating system was not adequate, can be ruled out based on following experiments. We increased CK to 320 units/ml in one set of ex-

periments, and CP to 25 mM in a second set, both at 20°C, and observed that K_1 did not change with these experimental manipulations (Zhao and Kawai, 1994). These results demonstrate that the standard CK (160 units/ml) and CP (15 mM) concentrations are adequate to regenerate ATP in rabbit psoas fibers. Thus, we conclude that the decrease of K_1 in the temperature range 5–20°C is not related to the ATP-regenerating system and that it reflects the genuine effect of ATP binding to cross-bridges.

In the high temperature range (20–30°C), the MgATP association constant (K_1) changes little (Fig. 5 *A*), indicating that the standard enthalpy change is small with the MgATP binding in this temperature range. This mechanism may be important for muscle to maintain continuous binding of ATP in all temperature ranges. Based on the observation that K_1 did not decrease as the temperature was elevated from 20 to 30°C, we infer that the CK concentration, which was increased to 320 units/ml at 25°C and to 640 units/ml at 30°C, was adequate in this temperature range.

The association constant for MgADP (K_0) changes similarly to K_1 (Fig. 5 *A*). This is expected, because MgADP is a competitive inhibitor of MgATP, and they occupy the same nucleotide-binding site on myosin (Cook and Pate, 1985; Schoenberg and Eisenberg, 1987; Kawai and Halvorson, 1989). In fact, we reported recently (Zhao and Kawai, 1994) that BDM has a large effect on the nucleotide-binding step, and its effect is similar in MgATP and in MgADP.

We were unable to resolve step 1b in the present report, because the data were scattered and there was a substrate inhibition on $2\pi d$ at 5–15°C. The observation that $2\pi d$ is least temperature-sensitive (Fig. 3) is consistent with an inference that both forward (k_{1b}) and backward (k_{-1b}) ATP-isomerization steps are not remarkably temperature-sensitive. This inference is based on the facts that, at high MgATP concentration (5 mM), $2\pi d$ is approximately the sum of k_{1b} and k_{-1b} (Eq. 29 of Zhao and Kawai, 1993), and that Q_{10} of $2\pi d$ is 1.5 (Table 1); hence Q_{10} of each step could not be very large. This conclusion is consistent with solution studies on S-1 or acto S-1 complexed with MgADP or MgAMPPNP (Trybus and Taylor, 1982). As is evident, the effect of temperature is least reliable for process (D) (hence step 1b) because of the frequency limitation of the present experimental apparatus. It is possible that this limitation caused the relative insensitivity of the apparent rate constant $2\pi d$ in the high temperature range (Fig. 3). The same problem may exist with Y_∞ (Fig. 1 *A*).

Cross-bridge detachment step

The rate constants of both cross-bridge detachment step 2 (k_2) and its reversal step (k_{-2}) increase with temperature (Fig. 5 *B*). Therefore, the equilibrium constant of the cross-bridge detachment step does not change significantly with temperature. Because the equilibrium constants, and not the rate constants, determine the probability of cross-bridges in tension-generating complexes (Eqs. 11 and 12), it can be concluded that the high temperature sensitivity of isometric tension is not related to the cross-bridge detachment step. It is interesting to note that there is little enthalpy or entropy change associated with the detachment reaction (Table 3).

Force-generation step

An interesting finding in the present study is that Pi-isomerization step 4 is the most temperature-sensitive step among the elementary steps in the cross-bridge cycle. This step corresponds to the force generation step (Kawai and Halvorson, 1991; Dantzig et al., 1992; Kawai and Zhao, 1993). This force generation step has been referred to as the "cross-bridge attachment step" in our previous publications, because the majority of cross-bridges in the Det state are truly detached under the current experimental condition. However, it may be more realistic to assume that the strongly attached AM*DP is formed via the weakly attached AMDP state (Brenner et al., 1991). The weakly attached cross-bridges are based on electrostatic interaction between segments of actin and myosin (Schoenberg, 1988; Sutoh et al., 1991; Rayment et al., 1993b).

In contrast to the large temperature effect of k_4, its reversal reaction (k_{-4}) is not very temperature-sensitive (Fig. 8). These results are consistent with those of Dantzig et al. (1992), who reported based on caged phosphate experiments at 10 and 20°C that the forward rate constant of the force-generating isomerization step has a higher temperature sensitivity than the backward rate constant. From Table 2, it is clear that the step that generates force has a high Q_{10} (6.8) and requires a considerable amount of activation energy (135 kJ/mol) (Table 2, Fig. 11). The high Q_{10} and activation energy required may imply that step 4 is a composite of multiple steps. These could include the hydrolysis step 3, the attachment step that results in a weakly attached state AMDP, and the force-generating isomerization step. In fact, the high temperature sensitivity of step 3 was demonstrated by solution studies of isolated S1 (Johnson and Taylor, 1978; Marston and Taylor, 1980). If this step is much faster than k_4, we will then observe the effect of these steps in k_4 with our methods. However, the hydrolysis step is known to occur at 100 s^{-1}

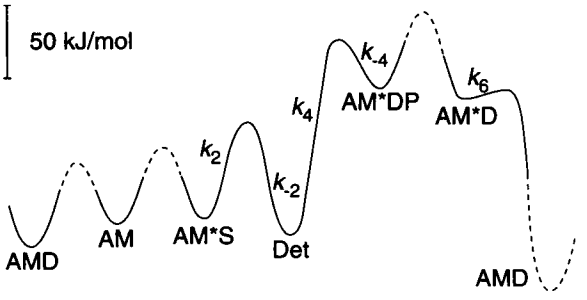

FIGURE 11 The reaction profile of the elementary steps, demonstrating activation energy and the enthalpy change. The profile is based on the parameters in Tables 2 and 3. Because the rate constants of steps 0, 1, and 5 were not measured, the presumed activation energy barrier is represented by the dotted line. Because the enthalpy change with step 6 was not measured, the level of AMD state is assumed.

in rabbit back and leg muscles at 20°C in solution (Johnson and Taylor, 1978), which is comparable with k_4 and k_{-4}, and this fact complicates the analysis.

Our results also demonstrate that the reversal reaction of step 4 does not require much activation energy (Table 2, Fig. 11). From this observation, we infer that the reversal step of force generation may not be an enzymatic reaction. This inference is consistent with our earlier conclusion based on a comparison of k_{-4} from cardiac muscle (Kawai et al., 1993) and from fast twitch skeletal muscle (Zhao and Kawai, 1993), demonstrating that k_{-4} was not much different between these two preparations.

Because the rate constant of force generation step (k_4) increases significantly with temperature, whereas the rate constant of its backward reaction (k_{-4}) does not change much, the equilibrium constant (K_4) increases significantly with temperature (Fig. 8). Therefore, the force generation step is an endothermic reaction and absorbs heat corresponding to 103 kJ/mol (Table 3). This observation is consistent with a large force increase with temperature increase in rabbit psoas fibers (Fig. 1 *A*; see also Goldman et al., 1987; Bershitsky and Tsaturyan, 1992; Davis and Harrington, 1993). In comparison, Tonomura et al. (1962) found that $\Delta H°$ = 240 kJ/mol for F-actin and myosin binding in solution, and Highsmith (1977) found that $\Delta H°$ = 44 kJ/mol for F-actin and S1 binding, indicating that an endothermic reaction is involved in the actin-myosin interaction. We further found that the force generation step accompanies a large entropy increase corresponding to 357 J/mol/deg (Table 3). When the free energy change ($\Delta G°$) is small, as in the case of the K_4 in our analysis (Eq. 16, Fig. 8), the large entropy increase is compensated for by the large enthalpy increase (Eq. 15). Therefore, it can be concluded that the force generation step in the cross-bridge cycle is an entropy-driven reaction.[1]

There are two general mechanisms for the large entropy increase. One mechanism is an increase in the soft internal vibrational modes between atoms, and the other mechanism is the change in the water structure associated with removal of hydrophobic residues from water (Highsmith, 1977; Sturtevant, 1977). Of these, we can rule out the first possibility, because the temperature of the experimental system is maintained. Therefore, an altered hydrophobic interaction seems to underlie the large entropy change. With a computerized docking analysis of actin and myosin (Rayment et al., 1993b), a possibility was raised that a stereospecific interaction occurs on myosin as a helix (Gly^{516}-Phe^{542})-loop (Pro^{543}-Thr^{546})-helix (Asp^{547}-His^{558}) motif, which comes close to actin residues Ile^{341}-Gln^{354} and Ala^{144}-Thr^{148}. The stereospecific interaction is primarily hydrophobic, and residues Pro^{529}, Met^{530}, Ile^{535}, Met^{541}, Phe^{542}, and Pro^{543} of myosin, and residues Ala^{144}, Ile^{341}, Ile^{345}, Leu^{349}, and Phe^{352} of actin are involved. Another hydrophobic interaction between segment Arg^{405}-Lys^{415} on myosin and Pro^{332}-Glu^{334} on actin is also possible. The formation of these interactions probably corresponds to step 4 in our analysis, because force is generated by step 4, and a large entropy increase is observed with this step. It has been known that large entropy increases are associated with formation of hydrophobic interactions in various enzyme systems (Sturtevant, 1977). These mechanisms are consistent with the interaction of actin and S-1 in solution, in which a large entropy increase corresponding to 280 J/mol/deg was observed (Highsmith, 1977); hence the reaction was entropy-driven and the interaction was hydrophobic in nature (Kodama, 1985).

Another possible structural change associated with force generation may relate to the conversion of an organized structure of a low entropy state into a freely jointed random coil of a high entropy state that generates force (Davis and Harrington, 1993). This mechanism is proposed because an increase in isometric tension does not always accompany an increase in stiffness. The results of the effect of temperature on isometric tension and stiffness showed that tension increase is greater than stiffness increase at high temperature (Fig. 1); other investigators generally obtained similar results (Ford et al., 1977; Bressler, 1981; Goldman et al., 1987). These results are consistent with the hypothesis that the tension supported by each cross-bridge may increase with an increase in temperature.

As is clear from Fig. 8, the equilibrium constant K_4 increases significantly with temperature. This will result in a significant increase in the number of cross-bridges in AM*DP and AM*D states, whereas the number of detached cross-bridges will decrease (Fig. 9). Because both AM*DP and AM*D states bear tension, tension will increase as a result of the temperature increase. This inference is consistent with our results in Fig. 1. Thus, we conclude that the large temperature sensitivity of the equilibrium constant of force generation step (K_4) is the major cause of the large temperature sensitivity of isometric tension.

Phosphate release step

Unlike the nucleotide-binding steps, which are sensitive to temperature, the Pi binding step (K_5) is not very sensitive to temperature (Fig. 8, Table 3). Our earlier studies showed that K_5 was little affected by osmotic compression (Zhao and Kawai 1993), TnC extraction (Zhao et al., 1994), or BDM treatment (Zhao and Kawai, 1994), whereas the nucleotide-binding step was affected by these experimental alterations. These results indicate that the Pi binding site on myosin is independent from the nucleotide-binding site and the contour of the Pi binding site does not change with the contour of the nucleotide binding site. According to our analysis as well as others, there is little change in the isometric tension with the Pi release (Kawai and Halvorson, 1991; Dantzig et al., 1992; Kawai and Zhao, 1993). Because the AM*DP state is unstable (low activation energy associated with k_{-4}, Table 2),

[1] Gilbert and Ford (1988) reached a similar conclusion by assuming that phase 2 of step analysis corresponds to the force generation step in frog sartorius muscles. In terms of our cross-bridge Scheme 1, their results can be interpreted as reversing steps 1 and 2, which would result in an endothermic reaction when the temperature is 20°C or less (Fig. 5).

the release of Pi may serve to stabilize the force generating complex. This situation is depicted in Fig. 11 by a dotted line.

Rate-limiting step

Our earlier studies demonstrated that step 6 is the slowest forward reaction in the cross-bridge cycle; hence it limits the ATP hydrolysis rate (Kawai and Halvorson, 1991; Kawai and Zhao, 1993). Otherwise, the effect of MgATP/MgADP on process (C) and the effect of Pi on process (B) could not be explained. We found that the ATP hydrolysis rate increased significantly with an increase in the temperature (Fig. 10). The increase in the ATP hydrolysis rate could be related to the increase in the cross-bridge number in the AM*D state, or to an increase in the rate constant k_6 (Eq. 3). Our analysis demonstrates that the increase is primarily based on an increase in the number of cross-bridges in the AM*D state, and not an increase in k_6 (Fig. 10). In other words, the rate constant of this rate-limiting step is not very temperature-sensitive, indicating that the activation energy of step 6 is very small (Table 2, Fig. 11). This fact is consistent with our previous hypothesis that step 6 is a mechanical step rather than a chemical step, and it occurs spontaneously (Kawai and Zhao, 1993). If the internal force generation corresponds to a chemomechanical process that results in the stretch of a spring, the external work performance corresponds to a mechanical process that results in the shortening of the spring. We propose here that the work is performed at step 6, because force is generated at step 4, and cross-bridges spend the longest time at step 6 (step 5 is brief). Evidently, ample time is essential to transduce the kinetic energy and the momentum, and to generate motion on an object (Kawai and Zhao, 1993).

Correlation of our results with temperature jump experiments

Cross-bridge Scheme 1 and the temperature sensitivity of the kinetic constants (Figs. 5 and 8) enable us to project the tension time course after a sudden change in temperature. When the temperature is increased, such as from 20 to 25°C, the major effect is an approximately twofold increase in k_4 (Fig. 8). The consequence of this increase is to promote steps 4 and 5 in Scheme 1. The result is an increased number of cross-bridges in the AM*D state (Fig. 9). Because K_5 decreases slightly (Fig. 8), which promotes step 5 further, the number of cross-bridges in the AM*DP state does not change much (Fig. 9). The cross-bridge number in the AM, AM*S, and Det states decreases to compensate for the increase in AM*D (Fig. 9). Because force generation occurs in step 4, an exponential rise of isometric tension with the rate constant defined by Eq. 5 will follow. This projection is in close agreement with results obtained by Davis and Harrington (1993). When the temperature was increased from 21 to 26°C, they observed an exponential rise of tension with the rate constant of 289 s^{-1} in rabbit psoas (their Fig. 1 *C*), which they named "medium speed relaxation ($1/\tau_2$)." The apparent rate constant calculated by Eqs. 5 and 6 with our kinetic constants (Figs. 5 and 8) and under their experimental conditions (~5 mM MgATP, ~1 mM endogenous Pi, 26°C) is 189 s^{-1}. Thus, it is apparent that Davis and Harrington's medium speed relaxation corresponds to step 4 in Scheme 1, which corresponds to process (B) in sinusolidal analysis, and to phase 3 in step analysis, and it does not correspond to phase 2 of step analysis as they assumed.

The amplitude of the fast transient corresponding to process (C) is small and would not be detectable with T-jump experiments, because the distribution of cross-bridges in the AM and AM*S states is small when the temperature is ≥20°C (Fig. 9), and also because K_1 and K_2 are not very temperature-sensitive in this range (Fig. 5). This projection is consistent with Davis and Harrington's observation that the fast speed relaxation was not detectable when the temperature was elevated to 26°C. Their "slow speed relaxation ($1/\tau_3$)" probably corresponds to process (A) observed in sinusoidal analysis. Our interpretation of this process is a sliding of thick and thin filaments (Tawada and Kawai, 1990), and it is not related to the rate-limiting step 6. The slowest step of the cross-bridge cycle could not be resolved in the transient analysis method. Davis and Harrington's observation was limited to the apparent rate constants, and they did not resolve the equilibrium constant; hence their results are not relevant to the discussion of enthalpy or entropy changes (see Eq. 15).

SUMMARY

From the present study, we observed that the elementary step 4 is the most temperature-sensitive step in the cross-bridge cycle. Because force is generated at step 4, our result is consistent with the large temperature sensitivity of the isometric tension. We found that a large entropy change is associated with step 4, implying that hydrophobic interaction between actin and myosin underlies the mechanism of force generation.

We express our great appreciation to Professors Charles A. Swenson, Sir Andrew F. Huxley, and Takao Kodama for their critical reading of the manuscript and useful suggestions.

This work was supported by grants from National Science Foundation DCB90-18096 and IBN 93-18120.

REFERENCES

Abbott, R. H., and G. J. Steiger. 1977. Temperature and amplitude dependence of tension transients in glycerinated skeletal and insect fibrillar muscle. *J. Physiol.* 266:13–42.

Bershitsky, S. Y., and A. K. Tsaturyan. 1989. Tension responses to joule temperature jump in skinned rabbit muscle fibres. *J. Physiol.* 447: 425–448.

Brenner, B., L. C. Yu, and J. M. Chalovich. 1991. Parallel inhibition of active force and relaxed fiber stiffness in skeletal muscle by caldesmon: implications for the pathway to force generation. *Proc. Natl. Acad. Sci. USA.* 88:5739–5743.

Bressler, B. H. 1981. Isometric contractile properties and instantaneous stiffness of amphibian skeletal muscle in the temperature range from 0 to 20°C. *Can. J. Physiol. Pharmacol.* 59:548–554.

Chase, P. B., D. A. Martyn, M. J. Kushmerick, and A. M. Gordon. 1993. Effect of inorganic phosphate analogues on stiffness and unloaded shortening of skinned muscle fibres from rabbit. *J. Physiol.* 460: 231–246.

Cook, R., and E. Pate. 1985. The effect of ADP and phosphate on the contraction of muscle fibers. *Biophys. J.* 48:789–798.

Dantzig, J., Y. Goldman, N. C. Millar, J. Lacktis, and E. Homsher. 1992. Reversal of the cross-bridge force-generation transition by the photogeneration of phosphate in rabbit psoas muscle fibers. *J. Physiol.* 451: 247–278.

Davis, J. S., and W. Harrington. 1987. Force generation by muscle fibers in rigor: a laser temperature-jump study. *Proc. Natl. Acad. Sci. USA.* 84:975–979.

Davis, J. S., and W. Harrington. 1993. A single order-disorder transition generates tension during the Huxley-Simmons phase 2 in muscle. *Biophys. J.* 65:1886–1898.

Eisenberg, E., and L. E. Greene. 1980. The relation of muscle biochemistry to muscle physiology. *Annu. Rev. Physiol.* 42:293–309.

Eastwood, A. B., D. S. Wood, K. L. Bock, and M. M. Sorenson. 1979. Chemically skinned mammalian skeletal muscle. I. The structure of skinned rabbit psoas. *Tissue and Cell.* 11:553–566.

Feldhaus, P., T. Fröhlich, R. S. Goody, M. Isakov, and R. H. Schirmer. 1975. Synthetic inhibitors of adenyl kinases in the assays for ATPases and phosphokinases. *Eur. J. Biochem.* 57:197–204.

Ford, L. E., A. F. Huxley, and R. M. Simmons. 1977. Tension responses to sudden length change in stimulated frog muscle fibres near slack length. *J. Physiol.* 269:441–515.

Geeves, M. A., R. S. Goody, and H. Gutfreund. 1984. Kinetics of acto-S1 interaction as a guide to a model for the cross-bridge cycle. *J. Muscle. Res. Cell Motil.* 5:351–361.

Gilbert, S. H., and L. E. Ford. 1988. Heat changes during transient tension responses to small releases in active frog muscle. *Biophys. J.* 54:611–618.

Goldman, Y. E., J. A. McCray, and K. W. Ranatunga. 1987. Transient tension changes initiated by laser temperature jumps in rabbit psoas muscle fibres. *J. Physiol.* 392:71–95.

Greene, L. E., and E. Eisenberg. 1980. Dissociation of actin·subfragment 1 complex by adenyl-5′-yl imidodiphosphate, ADP, and PPi. *J. Biol. Chem.* 255:543–548.

Güth, K., and R. Wojciechowski. 1986. Perfusion cuvette for the simultaneous measurement of mechanical, optical and energetic parameters of skinned muscle fibers. *Pflügers Arch.* 407:552–557.

Heinl, P., H. J. Kuhn, and J. C. Rüegg. 1974. Tension responses to quick length changes of glycerinated skeletal muscle fibres from the frog and tortoise. *J. Physiol.* 237:243–258.

Highsmith, S. 1977. The effects of temperature and salts on myosin subfragment-1 and F-actin association. *Arch. Biochem. Biophys.* 180: 404–408.

Huxley, A. F., and R. M. Simmons. 1971. Proposed mechanism of force generation in striated muscle. *Nature.* 233:533–538.

Johnson, K. A., and E. W. Taylor. 1978. Intermediate states of subfragment 1 and actosubfragment 1 ATPase: reevaluation of the mechanism. *Biochemistry.* 17:3432–42.

Kawai, M., and P. W. Brandt. 1980. Sinusoidal analysis: a high resolution method for correlating biochemical reactions with physiological processes in activated skeletal muscles of rabbit, frog and crayfish. *J. Muscle Res. Cell Motil.* 1:279–303.

Kawai, M., and H. R. Halvorson. 1989. Role of MgATP and MgADP in the cross-bridge kinetics in chemically skinned rabbit psoas fibers. Study of a fast exponential process (C). *Biophys. J.* 55:595–603.

Kawai, M., and H. R. Halvorson. 1991. Two step mechanism of phosphate release and the mechanism of force generation in chemically skinned fibers of rabbit psoas muscle. *Biophys. J.* 59:329–342.

Kawai, M., Y. Saeki, and Y. Zhao. 1993. Cross-bridge scheme and kinetic constants of elementary steps deduced from chemically skinned papillary and trabecular muscles of the ferret. *Circ. Res.* 73:35–50.

Kawai, M., and Y. Zhao. 1993. Cross-bridge scheme and force per cross-bridge state in skinned rabbit psoas muscle fibers. *Biophys. J.* 65: 638–651.

Kodama, T. 1985. Thermodynamic analysis of muscle ATPase mechanisms. *Physiol. Rev.* 65:467–551.

Kuhn, H. J. 1981. The mechanochemistry of force production in muscle. *J. Muscle Res. Cell Motil.* 2:7–44.

Marston, S. B., and E. W. Taylor. 1980. Comparison of the myosin and actomyosin ATPase mechanisms of the four types of vertebrate muscles. *J. Mol. Biol.* 139:573–600.

Meyer, R. A., T. R. Brown, and M. J. Kushmerick. 1985. Phosphorus nuclear magnetic resonance of fast- and slow-twitch muscle. *Am. J. Physiol.* 248: C279–C287.

Rall, A. J., and R. C. Woledge. 1990. Influence of temperature on mechanics and energetics of muscle contraction. *Am. J. Physiol.* 259:R197–R203.

Ranatunga, K. W., and S. R. Wylie. 1983. Temperature-dependent transitions in isometric contractions of rat muscle. *J. Physiol.* 339:87–95.

Rayment, I., H. M. Holden, M. Whittaker, C. B. Yohn, M. Lorenz, K. C. Holmes, R. A. Milligan. 1993b. Structure of the actin-myosin complex and its implications for muscle contraction. *Science.* 261:58–65.

Rayment, I., W. R. Rypniewski, K. Schmidt-Bäse, R. Smith, D. R. Tomchick, M. M. Benning, D. A. Winkelmann, G. Wesenberg, and H. M. Holden. 1993a. Three-dimensional structure of myosin subfragment-1: a molecular motor. *Science.* 261:50–58.

Schoenberg, M. 1988. Characterization of the myosin adenosine triphosphate (M. ATP) crossbridge in rabbit and frog skeletal muscle fibers. *Biophys. J.* 54:135–148.

Schoenberg, M., and E. Eisenberg. 1987. ADP binding to myosin cross-bridge and its effect on the cross-bridge detachment rate constants. *J. Gen. Physiol.* 89:905–920.

Sturtevant, J. M. 1977. Heat capacity and entropy changes in processes involving proteins. *Proc. Natl. Acad. Sci. USA.* 74:2236–2240.

Sutoh, K., M. Ando, K. Sutoh, and Y. Yano-Toyoshima. 1991. Site-directed mutations of Dictyostelium actin: disruption of a negative charge cluster at the N terminus. *Proc. Natl. Acad. Sci. USA.* 88:7711–7714.

Szilagyi, L., M. Balint, F. A. Sréter, and J. Gergely. 1979. Photoaffinity labelling with an ATP analog of the N-terminal peptide of myosin. *Biochem. Biophys. Res. Commun.* 87:936–945.

Takashi, R., and S. Putnam. 1979. A fluorimetric method for continuously assaying ATPase: application to small specimens of glycerol-extracted muscle fibers. *Anal. Biochem.* 92:375–82.

Tawada, K., and M. Kawai. 1990. Covalent cross-linking of single fibers from rabbit psoas increases oscillatory power. *Biophys. J.* 57:643–647.

Taylor, E. W. 1979. Mechanism of actomyosin ATPase and the problem of muscle contraction. *CRC Crit. Rev. Biochem.* 6:103–164.

Tonomura, Y., S. Tokura, K. Sekiya. 1962. Binding of myosin A to F-actin. *J. Biol. Chem.* 237:1074–1081.

Tregear, R. T., and J. M. Squire. 1973. Myosin content and filament structure in smooth and striated muscle. *J. Mol. Biol.* 77:279–290.

Trybus, K. M., and E. W. Taylor. 1982. Transient kinetics of adenosine 5′-diphosphate and adenosine 5′-(β,γ-imidotriphosphate) binding to subfragment 1 and actosubfragment 1. *Biochemistry.* 21:1284–1294.

Zhao, Y., and M. Kawai. 1992. The effect of temperature on the elementary steps of the cross-bridge cycle in rabbit psoas fibers. *Biophys. J.* 61:267*a*. (Abstr)

Zhao, Y., and M. Kawai. 1993. The effect of lattice spacing change on cross-bridge kinetics in chemically skinned rabbit psoas muscle fibers. II. Elementary steps affected by the spacing change. *Biophys. J.* 64:197–210.

Zhao, Y., and M. Kawai. 1994. BDM affects nucleotide binding and force generation steps of the cross-bridge cycle in rabbit psoas muscle fibers. *Am. J. Physiol.* 266:C437–C447.

Zhao, Y., P. M. G. Swamy, and M. Kawai. 1994. Effect of partial extraction of troponin C on elementary steps of the cross-bridge cycle in skinned rabbit psoas muscle fibers. *Biophys. J.* 66:303*a*. (Abstr.)